DELAMINATION IN ADHESIVELY BONDED CFRP JOINTS: STANDARD FATIGUE, IMPACT FATIGUE AND INTERMITENT IMPACT

J.P. Casas-Rodriguez, I.A. Ashcroft and V. V. Silberschmidt,

Wolfson School of Mechanical and Manufacturing Engineering
Loughborough University, Leicestershire LE11 3TU

Keywords:
A. Adhesive joints, A. Carbon fibre, B. Fatigue, B. Impact behaviour, C. Damage tolerance.

Abstract

The response of adhesive joints to three fatigue regimes, namely; constant amplitude sinusoidal loading (standard fatigue, SF), cyclic in-plane impacts (impact fatigue, IF) and a combination of the two (CSIF), has been investigated. The samples used in this study were carbon fibre reinforced polymer (CFRP) lap-strap joints (LSJs) bonded with a rubber modified epoxy adhesive. It was observed that fatigue fracture at very low load amplitudes occurred in IF. Two main patterns of failure were observed in SF; cohesive failure in the adhesive, which was linked to slow fatigue crack growth behaviour, and a mixed-mode failure, involving failure in both the adhesive and the CFRP. In addition, it was observed that the transition from cohesive to mixed mode failure was accompanied by crack growth acceleration. In IF it was seen that all failure was of a mixed-mechanism nature. In the combined standard and impact fatigue it was seen that the introduction of a relatively small number of impacts between SF blocks drastically changed the dynamics of fatigue crack propagation, increasing the crack rate. A further observation was that cavitation of rubber particles in the adhesive, which is seen as evidence of active toughening, was affected by the addition of impact loading.

1. Introduction

In recent decades, the aerospace and automotive industries have been characterized by a continuing increase in the use of carbon fibre-reinforced polymer (CFRP) in structural applications. These developments have necessitated a thorough analysis of

fatigue in CFRPs. Records of time-load histories of various components and structures have shown that they are exposed to a variety of cyclic loads that vary through the structure. In some cases, repeated low-energy impacts appear in the load spectrum. This phenomenon is known as "impact-fatigue" and it has been shown that this type of loading can be far more damaging than SF [1].

Analysis of impact-fatigue in CFRPs has been principally aimed at characterising the reduction in fatigue life as the load is increased. It was found in a cyclic charpy test of jute/vinyl-ester composite that there was an increase in the fatigue endurance as the impact energy decreased [2]. Some researchers [3,4] have also identified a threshold energy of impacts, below which no visible delamination is observed; and concluded it was in [5] that the response to impact loading depends on the orientation of fibres in CFRP.

The fatigue life of CFRP laminates was investigated in [6] where sinusoidal in-plane loads were combined with a single out-of-plane impact. It was found that the fatigue strength of the CFRP was affected by the sequence, with the effect being more pronounced in the case when the sinusoidal load followed the impact than in the converse sequence. Similar experiments have been performed with a glass fibre-reinforced composite [7], where it was found that a simple out-of-plane impact had a significant effect on the fatigue life and that this behaviour was strongly related to the post-impact residual strength.

Various techniques have been considered to produce joints between CFRP parts; the most popular being mechanical fasteners (nuts, screws, rivets, etc.) and adhesive joints. The comparative advantages of these two techniques have been analysed in [8]. It is commonly accepted that adhesive joints are characterized by their low weight and a potential reduction in stress concentrations in comparison to mechanical fasteners. However, adhesive joints can be seriously affected by environmental ageing [9].

Structural adhesives can be considered as nano-composites [10] as they are typically multi-components materials. Structural adhesives commonly use epoxy resins as a matrix with rubber particles and/or inorganic fillers [11] to generate a toughening mechanism. Extensive research has been undertaken to study the effect of

these inclusions on the epoxy matrix. This effect can be summarized in terms of three mechanisms [12]. The first is the cavitation of rubber particles. This mechanism is characterized by the presence of holes in the fracture surface of the adhesive. A second mechanism is the formation of shear bands. This can occur in areas with a high number of rubber particles, increasing the possibility of the onset of plasticity. A third mechanism is rubber bridging in which the rubber particles bridge a gap in the fractured surfaces, thus impeding crack propagation. These mechanisms are dependent on the volume fraction and size of rubber particles [10].

The current state of research into in-plane cyclic impacts of adhesive joints with CFRP composites used as adherends is characterised by a lack of experimental studies of the many facets of this phenomenon. The main aim of this paper is to investigate the behaviour of bonded CFRP lap-strap joints subjected to three loading regimes: standard fatigue, impact fatigue and a combination of impact and standard fatigue.

2. Experimental setup

2.1 Sample preparation

Samples for the experimental studies were manufactured by adhesive bonding cured panels of CFRP. The composite used was T800/5245C, supplied by Cytec Ltd. The matrix, Rigidite 5245C, is a modified bismaleimide/epoxy system and is reinforced with T800 fibres supplied by Toray Industries Ltd. The composite panels were laid-up from unidirectional (UD) pre-preg with a volume fraction of 0.6 and thickness of 0.125 mm. A multidirectional (MD) lay-up scheme of $[(0/-45/+45/0)_2]_S$ was used and the panels were cured for 2 hours at 182ºC with an initial autoclave pressure of approximately 600 kN/m^2. The cured panels were ultrasonically scanned to detect defects. The material properties for the tested MD panels are given in Table 1, as calculated from the UD properties using laminate theory [13]. The adhesive used was Hysol Dexter's EA-9628, which was supplied as a 0.2 mm thick film. This adhesive is based on a diglycidyl ether of bisphenol A with a primary amine curing agent. A reactive liquid polymer, based on carboxyl terminated butadiene acrylonitrile rubber, was used as a toughening agent. The material properties for EA-9628 are given in Table 2.

The lap-strap joints (LSJ) (see Fig. 1 for dimensions) were assembled using pre-cured CFRP laminate panels and sheets of EA-9628 adhesive. The adhesive was cured in an autoclave for 60 min at 120ºC. The final samples were obtained by cutting the bonded panels using a diamond saw. End tabs for the specimens were made of 7075-T6 aluminium alloy and bonded with FM-73 adhesive. Holes were drilled in the specimens used for the IF and CISF tests using three drills with different diameters to minimise the possibility of delamination in the composite.

Table 1

Mechanical properties of T800/5245C composite at room temperature

	E_x (GPa)	E_y (GPa)	G_{xy} (GPa)	ν_{xy}	ν_{yx}
UD	174	9.64	7	0.36	0.02
MD	99.8	28.1	25.7	0.69	0.2

Table2

Mechanical properties of EA-9628 at room temperature

Yung's Modulus (GPa)	Yield stress (MPa)	Ultimate stress (MPa)	Strain to failure (%)
2.01	29	57.7	10.4

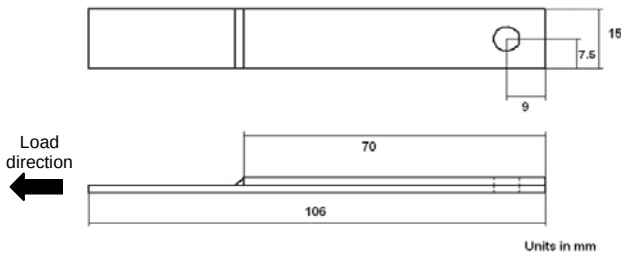

Fig. 1 Dimensions of lap-strap joint specimens

2.2 Quasi-Static and Standard Fatigue tests

A servo-hydraulic fatigue testing machine, using digital control and data logging, was used in the quasi-static, SF and CISF tests. The quasi-static failure load was calculated as the average of the maximum force reached by two specimens tested at a displacement rate of 0.05 mm/s. SF was investigated by testing two specimens in force control with a sinusoidal waveform, load ratio (minimum to maximum load) of R= 0.1 and frequency of 5 Hz. The maximum load was selected as 60% of the quasi-static failure load. Tests were performed in ambient laboratory conditions. Thermocouples were placed at various points on the surfaces of the samples in order to investigate any thermo-elastic effects during testing, however, no change in temperature was observed.

2.3. Impact-Fatigue Tests

IF tests were carried out on 7 specimens using a modified CEAST RESIL impactor, as described in detail in [1]. In these experiments a specimen is fixed at one end to an instrumented vice and a special impact block is attached to its free end (Fig. 2). The impact of the pendulum hammer produces a tensile load in the specimen for a short interval. In the IF test the pendulum hammer is released from a pre-selected initial angle. This angle is kept constant during the entire test, corresponding to an initial potential energy of 1.07 J and impact velocity of 1.9 m/s. The time between impacts was approximately 15 seconds.

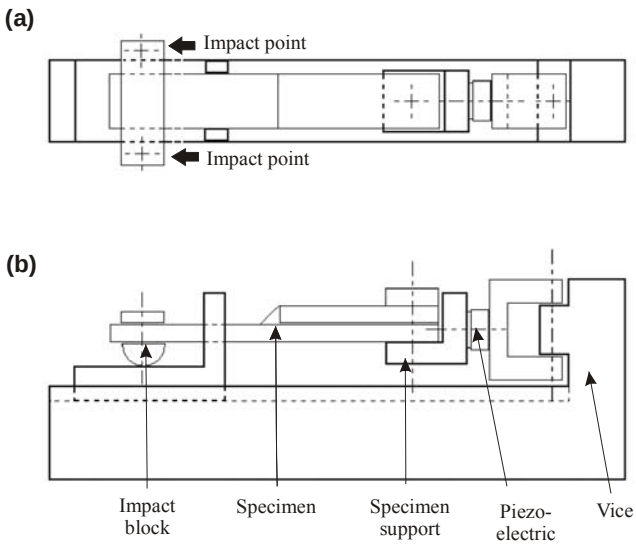

Fig. 2 Sample set-up for impact-fatigue. (a) Plan view, (b) side view.

2.4 Combined Impact and Standard Fatigue (CISF)

The CISF test is an intermittent sequence; consisting of two types of loading blocks. The first block consists of 100 tensile-impacts, as described in section 2.3. The second block consists of 5000 sinusoidal cycles, similar to those described in section 2.2. Two specimens were tested in this manner.

2.5 Fatigue crack growth

The process of fatigue crack growth in SF was examined by means of in-situ crack measurements. A system of marks was produced with a Vernier calliper on the white painted surface of the specimens' edge as a reference for all specimens. The crack size was then measured using portable optical microscopy for both edges in all specimens. Measurements of crack lengths in the IF tests were carried out using optical microscopy; with computer controlled halting of the test after a prescribed number of impacts so that the specimen could be studied. Captured digital images were used to measure the crack size.

2.4 Fractography

After testing, fracture surfaces were examined with an optical microscope. High-magnification studies were also performed using a scanning electron microscope (SEM). Samples were gold coated prior to SEM examination and a voltage range of 15-25 kV was used.

3. Results and discussion

3.1 Standard fatigue

Analysis of the fracture surfaces in SF has shown the presence of two main macro-mechanisms of failure. The first SF specimen (SF1) exhibited predominantly cohesive failure in the adhesive layer (from herein simply termed 'cohesive failure') over the entire fracture surface. SEM of the strap fracture surface (Fig. 3) shows a typical fracture surface. The fracture surface exhibited ductile tearing, voiding and cavitation of rubber particles [10,12]. The 'wavy' fracture surface indicates a mixed-mode fracture process.

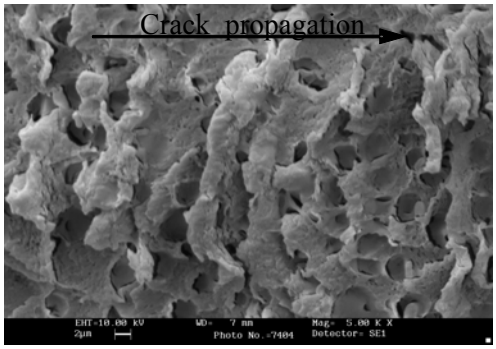

Fig. 3 Detail of the cavitated rubber particles in specimen tested in SF with a cohesive failure

A more complex mechanism of failure was seen in the second standard fatigue specimen (SF2), similar to that described in previous studies [14]. Three different regions were identified in the fracture surface, as seen in Fig. 4. The first region (region I in Fig. 4) corresponds to cohesive failure in the adhesive layer. A second region (region II in Fig. 4) is a transition region, in which a mixture of failure in the adhesive and in the 0º ply of the CFRP, adjacent to the adhesive, is seen. In region III, the failure process is dominated by fracture in the CFRP ply adjacent to the adhesive.

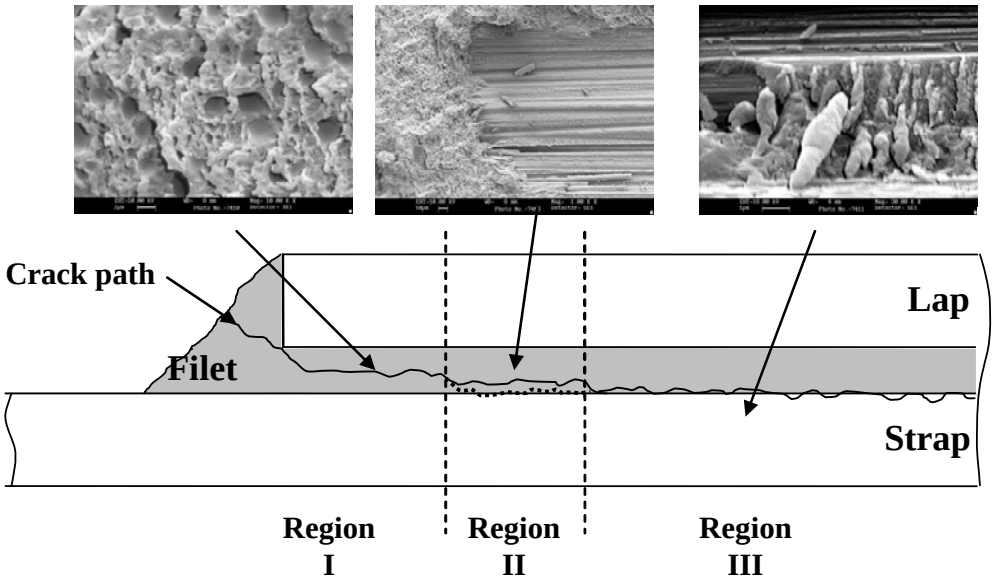

Fig. 4 Crack propagation in standard fatigue

SEM analysis of region I was similar to the fracture surface seen in SF1. Region II is characterized by a transition from failure in the adhesive to failure in the CFRP. It was observed that these changes were not constant along the crack

delamination front; instead intermittent bands with different lengths were seen. Failure in the CFRP material was located predominantly in the 0º ply adjacent to the adhesive. It can be seen in Fig. 4 that this fracture is a mix of failure in the matrix of the composite and fibre debonding. Rollers and plastically deformed shear cusps can be seen in the areas of matrix failure. Shear cusps, related to mode II loading can be seen and in some cases these cusps have been transformed to matrix rollers due to the effect of the continuous fretting of the surface in fatigue. Some fibre breakage is also seen in the fracture surface; however, the main crack front does not break through the fibres and hence remains in the plane parallel to the ply adjacent to the adhesive.

The various regions of the fracture surface can be related to variations in the fatigue crack growth (FCG) behaviour, shown in Fig. 5. Comparison of Figs. 4 and 5 shows that cohesive fracture (SF1) is associated with a relatively slow crack growth, resulting in a large number of cycles to failure. In contrast, an accelerated FCG rate is associated with failure in the composite. Fig. 6 shows a comparison of the crack growth rates in the two specimens which emphasises the accelerating effect of the fracture shifting to the composite substrate. The crack propagation rate in the initial stages is around 3×10^{-4} mm/cycle for both specimens. After this, crack acceleration is observed in SF2 corresponding to the crack entering region II. Conversely, cohesive failure in SF1 is characterized by a continuing decline in the crack growth rate over the entire life of the specimen.

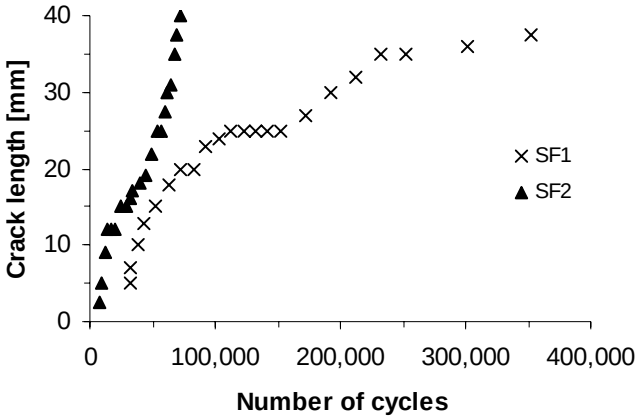

Fig 5. Crack growth in standard fatigue.

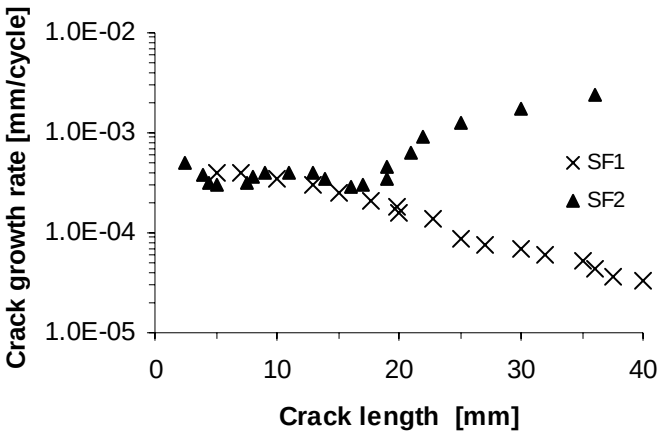

Fig. 6. Crack growth rate in standard fatigue.

3.2 Impact Fatigue

Initial optical examination of specimens tested under IF conditions showed patterns of failure similar to those observed in SF2, as seen in Fig. 7. the first region shows cohesive failure in the adhesive, followed by a transition region with a mixture of adhesive and CFRP fracture; and finally, a third region where the crack grows in the 0º composite ply adjacent to the adhesive.

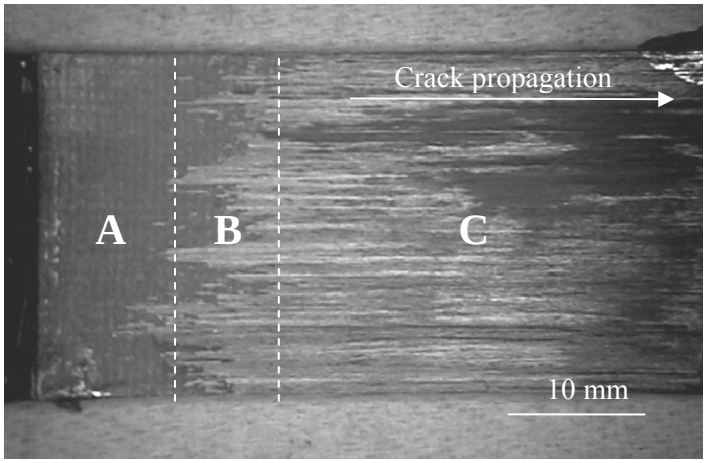

Fig. 7 Failure surface of a sample tested in impact-fatigue [IF5 specimen]

However, a more detailed analysis shows distinct differences between the fracture surfaces in IF and SF. It should also be emphasised that IF specimens have been tested with peak loads of approximately 11% of the quasi-static failure load of the joint (as compared to 60% for SF). It is seen that even at this load level a

considerable amount of damage is seen in the joint after relatively few cycles. It was found that eventual failure, was detected in some IF specimens (particularly IF6 and IF7) at very low numbers of cycles in comparison to the test in SF with a similar facture path. A general analysis of the FCG under IF conditions in Fig. 8 shows that the results can be divided into two main groups, based on the FCG behaviour. A very rapid FCG was found in two specimens (IF6 and IF7). A reliable crack growth rate for IF6 could not be obtained because of the low number of impacts; however, a crack growth rate of approximately 10^{-2} mm/cycle was calculated over the entire fatigue life of IF7, as shown in Fig. 9. A more mixed FCG behaviour was found in the other five IF specimens. A general trend for these specimens was an initial crack speed of approximately 10^{-2} mm/cycle until a crack length of around 10 mm was reached. After that a decrease in the crack growth rate was seen. This decreasing trend changed when the crack reached a length of approximately 27 mm, when a constant rate plateau was observed. This was between 10^{-3} mm/cycle and 2×10^{-5} mm/cycle. Differences in the crack speed were also detected for IF and SF tests. Comparison of Figs. 6 and 9 shows that the crack propagation rate in the initial stages of failure in IF was significantly higher than in the initial stages of failure in SF.

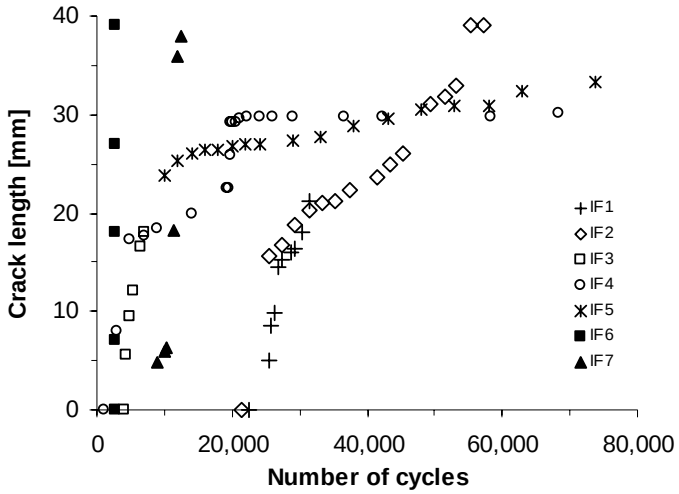

Fig. 8 Crack growth in impact-fatigue

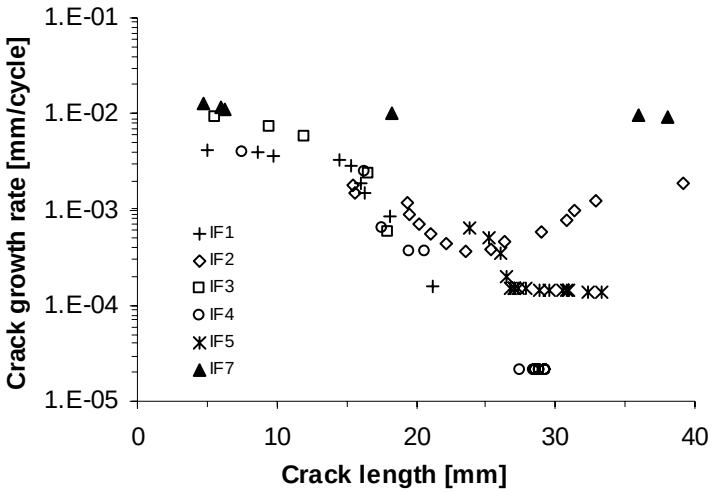

Fig. 9 Crack growth rate in impact fatigue

As noted above, it was seen in the IF specimens that the fracture behaviour involved three regions. These regions can be described as; predominantly cohesive failure (region A), a mix of cohesive failure and composite matrix failure (region B) and failure predominantly in the CFRP ply adjacent to the adhesive (region C). However a deviation from the general behaviour was seen in specimen IF2 where the failure in region C combined delamination between 0º and 45º plies at the specimen edges and failure in the 0º layer adjacent to the adhesive in the middle of the sample. The may explain the acceleration in FCG for IF2 in region C shown in Fig. 9.

SEM analysis of region A for sample IF7 revealed that this failure is characterized by a lack of cavitating rubber particles, as shown in Fig. 10. Previous work [16] has found that in unstable fracture regions (i.e. fast FCG) rubber particles can remain intact, resulting in an indistinct difference between the epoxy matrix and the rubber. It was shown in [17] that under certain load conditions the cavitation process can be suppressed; no differences in the fracture toughness between modified and unmodified epoxy were found in that case. This behaviour was explained as a consequence of the decrease of the shear banding effect due to insufficient levels of plastic deformation caused by the rubber particles.

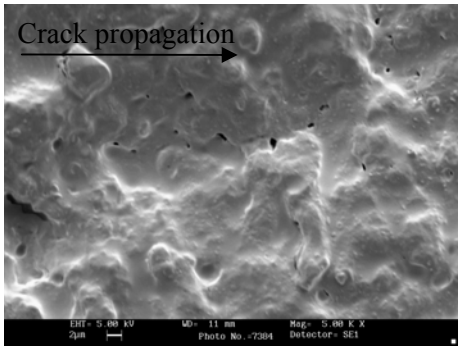

Fig. 10 Fracture in region A in specimens tested in IF conditions with fast crack growth [IF7 specimen]

Analysis of region B in IF7 shows that this region exhibits non-homogenous fracture behaviour, as illustrated in Fig. 11-a. This is characterised by the presence of "islands", i.e. changes in the fracture path, when a crack suddenly changes from cohesive failure to damage in the composite and later returns to cohesive failure of the adhesive. This behaviour can be explained by the nucleation of micro cracks in front of the main crack front, generating a local pattern of failure that in time becomes merged with the main crack. Previous studies [14] based on X-ray radiography for a similar type of specimens, have shown small regions of secondary debonding ahead of the main crack that can cause this behaviour. In region C damage occurs predominantly in the composite-matrix ply adjacent at the adhesive. Fracture in the matrix demonstrates a brittle character, with none of the rollers found in SF.

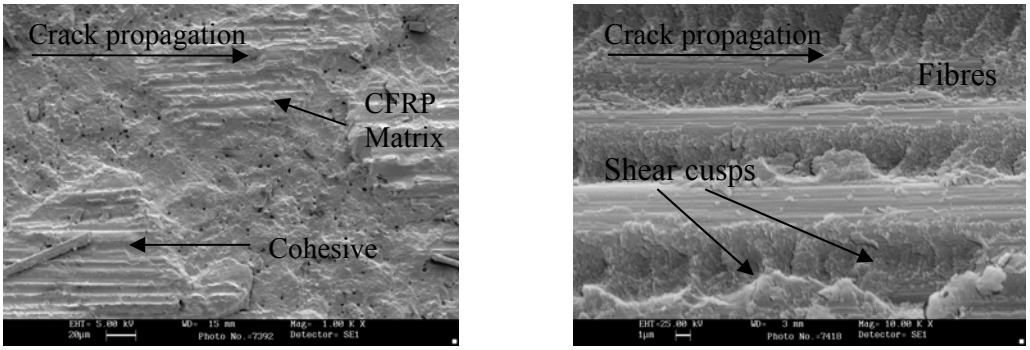

(a) **(b)**

Fig. 11 Failure in IF specimens with fast FCG behaviour [IF7 specimen]: (a) details of failure in region B of the lap; (b) details of failure in region C

Slow crack growth in IF was seen in two specimens (IF4 and IF5 in Figure 8) when the crack reached a length between 15 and 25 mm. This behaviour can be

explained by a change of the FCG mechanisms. Fig. 12-a shows a fracture surface in region A of IF5 and although voiding is seen, there are no signs of rubber cavitation. The fracture surface in region B showed signs of multiple damage initiation and termination sites. In some areas there are imprints of fibres on the fracture surface indicating that damage is close to or in the composite but then returns to the adhesive layer (Fig. 12-b). Micrographs from region C of the IF fracture surface are presented in Figs. 12-c and d. It can be seen that the fracture of fibres is far more common than in the case of SF. Also, as with the cohesive failure in IF, the fracture surface is less uniform than that for SF and shows signs of multiple damage events. Fracture in the composite matrix can be observed more clearly in Fig. 12-c. In contrast to the fast FCG in IF, shear cusps can be seen randomly distributed over the matrix. However, the matrix demonstrates a general brittle behaviour, as seen in Fig. 12-d.

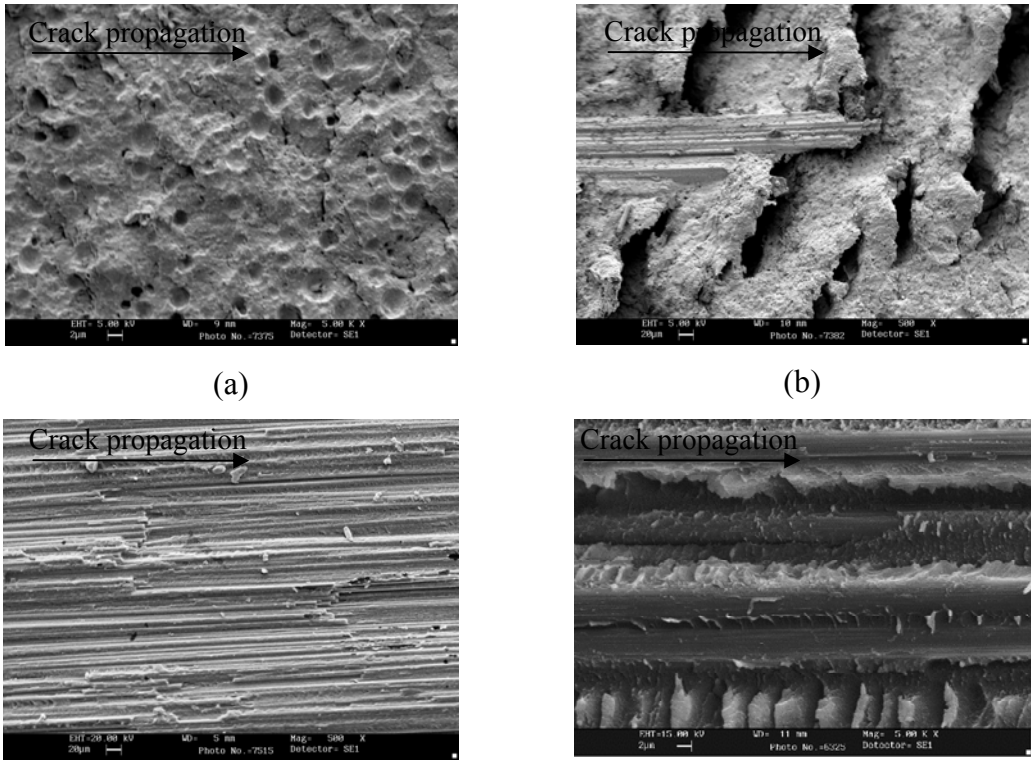

Fig. 12 SEM of fracture surfaces from samples tested in IF with a slow FCG behaviour [IF5 specimen]. (a) Region A, (b) Region B over the lap, (c) and (d) region C.

3.3 Combined impact and standard fatigue

In the case of combined impact and standard fatigue (CISF), studies of the crack growth and fracture surfaces revealed two main mechanisms of failure, which are

similar to those discussed above. A fast FCG is associated with an intermittent adhesive-CFRP failure mechanism (specimen CISF1) and a slow FCG with predominantly cohesive failure (CISF2). A comparison of FCG for specimens with fast failure in CISF and SF is shown in Fig. 13. It can be seen that in CISF, stable crack growth behaviour is observed until the crack reaches a length of 10mm, when the FCG becomes unstable. Analysis of the fracture surfaces show that this crack length corresponds to a change from region A to region B. All the stages of the crack growth process in CISF start considerably earlier in the specimen's life than in SF with the eventual failure occurring at a number of cycles that is nearly an order of magnitude lower.

Results of SEM performed for the fast FCG specimen tested in CISF conditions are presented in Fig. 14. Analysis of region A (Fig. 14-a) shows a considerable number of cavitating rubber particles, demonstrating that the toughening effect is active before the onset of unstable the crack growth. In addition, a significant amount of broken fibres were observed, these being more common near to the boundary between regions B and C. Matrix damage in the ply adjacent to the adhesive was characterized by the presence of small, poorly developed shear cusps instead of the well developed, plastically deformed shear cusps seen in SF. Additional studies of the crack rate in a fast CISF specimen demonstrates the drastic change between IF and SF. In the SF blocks the FCG rate was approximately 10^{-3} mm/cycle, whereas in the IF blocks rates of approximately 2.2×10^{-2} mm/cycle were seen.

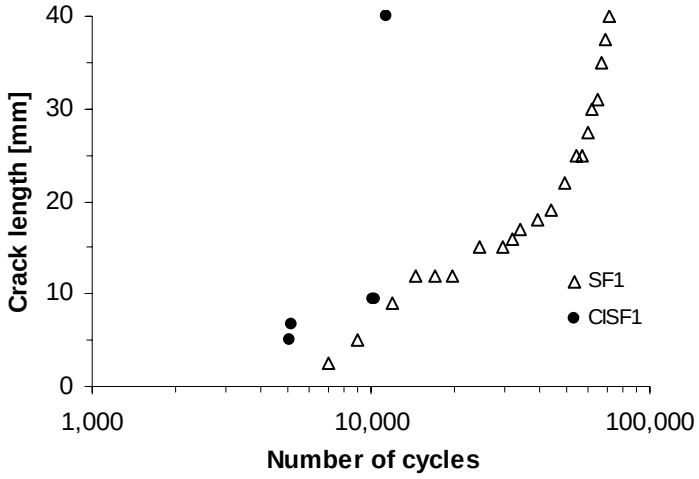

Fig. 13 Comparison of FCG in specimens tested in CISF and SF with intermittent adhesive-CFRP failure

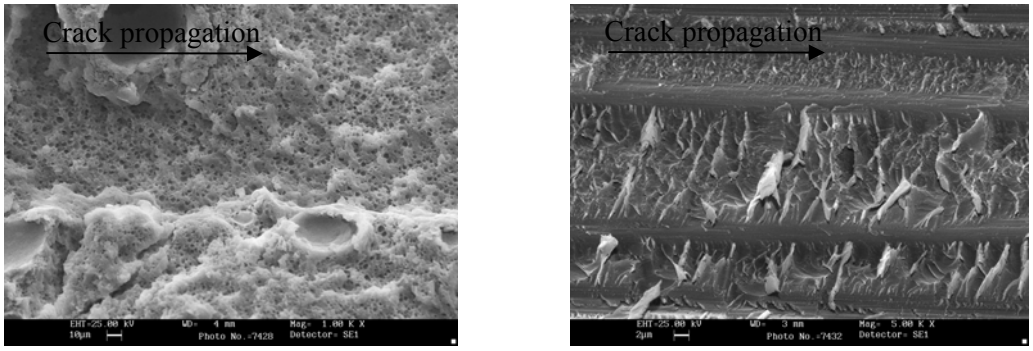

(a) (b)

Fig. 14 SEM of fracture surfaces in samples tested in CISF with a slow FCG behaviour (a) region A, (b) region C

Slow FCG behaviour in CISF (CISF2) is compared with cohesive failure in SF in Fig. 15. A general analysis of the crack rate reveals the very strong effect of a relatively small number of in-plane impacts on the dynamics of fatigue when cohesive failure is observed in the adhesive. It was found that the crack rate tended to decrease until a crack size of around 15 mm was reached. Then a transition occurred to a practically constant average value of the crack growth rate at a level of approximately 8×10^{-3} mm/cycle until eventual failure. The figure also shows that the crack growth rate in the IF bocks tended to be higher than that in the SF blocks, even though the peak loads were considerably lower in the former.

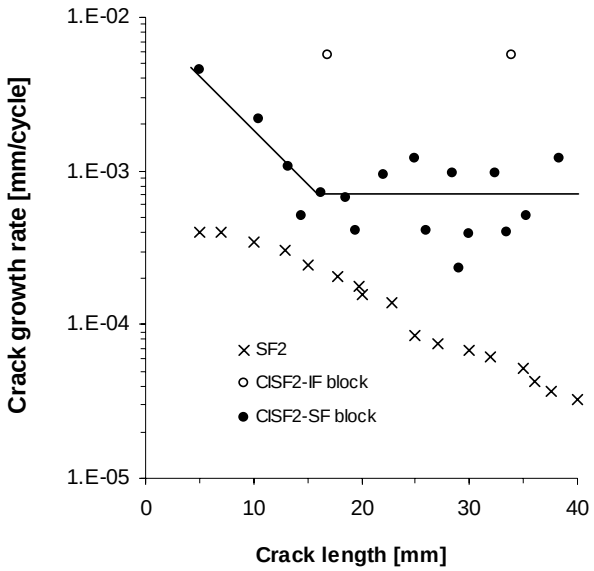

Fig. 15 Comparison of crack rate in CISF and SF for slow crack growth specimens

SEM analysis of the fracture surfaces of the CISF samples revealed that the IF blocks affected the uniformity of the fracture surface, as illustrated in Fig. 15-b. Changes in the failure mechanism are concentrated in localised areas and are characterized by the presence of small valleys where no cavitating-rubber particles are present. Additional studies showed that the toughening mechanism characterised by rubber cavitation is active during the SF blocks of the test, but results in a more irregular distribution of cavities than in pure SF. This mechanism of failure can be explained by the fact that the crack growth depends on the loading history, being affected by the damage zone ahead of the crack front, where micro-damage can exist.

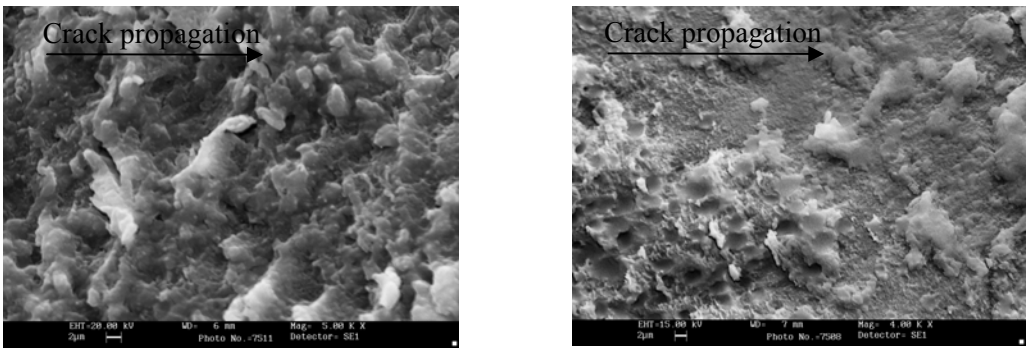

(a) (b)

Fig. 15 SEM of fracture surfaces in specimens tested in CISF with a cohesive failure: (a) SF region, (b) IF region.

4. Conclusions

Fatigue in adhesively bonded CRFP LSJs was studied in this paper. It can be concluded from these tests that cyclic in-plane tensile impacts are far more damaging than standard non-impact fatigue. It is found that significant fatigue damage is present in IF conditions at relatively low fractions of the quasi-static strength compared with SF.

Two typical patterns of failure were seen; a cohesive failure in the adhesive, that is related to slow fatigue crack growth, and a mixed-mechanism failure that is associated with fast fatigue crack growth. It was also seen that a change in the pattern of failure from cohesive to the mixed-mechanism path acted an accelerator of the crack growth in specimens tested in SF. In IF a mixed-mechanism path was seen in all samples tested. Differences between IF and SF were also seen with regard to the crack

speed. It was found that in the initial stages of the crack propagation, the crack rate is 10 times higher in IF than in SF.

It was found that the introduction of a relatively small number of in-plane impacts between blocks of SF drastically changes the dynamics of fracture in the specimen, with the IF blocks having a damage accelerating effect.

It was also observed that the toughening mechanism of the rubber particles present in the adhesive was affected by cyclic in-plane impacting. The rapid crack growth in the adhesive associated with impact fatigue was characterised by a lack of rubber particle cavitation.

References

1. Casas-Rodriguez J.P., Ashcroft, I.A. and Silberschmidt V.V., *Damage evolution in adhesive joints subjected to impact fatigue*, Int. J. Sound Vibra. in press.

2. Ray D., Sarkar B.K., Bose N.R., *Impact fatigue behaviour of vinylester resin matrix composites reinforced with alkali treated jute fibres*. Compos. Part A. 2002; 33: 233-241

3. Khan B., Rao R.M.V.G.K, Venkataraman N. *Low velocity impact fatigue studies on glass epoxy composite laminates with varied material and test parameters – effect of incident energy and fibre volume fraction.* J. Reinf. Plast. Compos. 1994;14:1150-1159

4. Sinmmazçelik T., Armağan A., *Impact-fatigue behaviour of unidirectional carbon fibre reinforced polyetherimide (PEI) composites*. J. Mater. Sci. 2006; 41:6237-6244

5. Yuan Q., Friedrich K., Karger-Kocsis J., *Low-energy charpy impact of interleaved CF/EP laminates.* Appl. Compos. Mat. 1995; 2:119-133

6. Ding Y.Q., Yan Y., McIlhager R., *Effect of impact and fatigue loads on the strength of plain weave carbon-epoxy composites*. J. Mater. Process. Technol. 1995;55:58-62

7. Yuanjian T., Isaac, D.H., *Combined impact and fatigue of glass fibber reinforced composites*, Compos: Part B 200, doi: 10.1015/j.compositesb.2007.03.005

8. Schön J., Strarikoc R., *Fatigue of joints in composite structures.* In: Harris B., editor. Fatigue in composites; Woodhead Publishing Limited, (2003), pp 621-643

9. Ashcroft I.A. Hughes D.F., Shaw S.F., *Adhesive bonding of fibre reinforced polymer composite materials.* Assembly Autom. 2000; 20:150-161

10. Isik I., Yilmazer U., Bayram G. *Impact modified epoxy/montmorillonite nancomposited: systhensis and characterization*. Polymer 2003; 44: 6371-6377

11. Azimi H.R., Pearson R.A., Hertzberg R.W., *Fatigue of hybrid epoxy composited: epoxies containing rubber and hallow glass spheres*. Polymer Eng. Sci 1996; 36: 2352-2365

12. Kinloch A J. *Adhesives in engineering.* P I Mech Eng G-J AER 1997; 211:307-335

13. Ashcroft I.A. Abdel Wahab M.M., Crocombre A.D., Hughes D.J., Shaw S.J., *The effect of environment on the fatigue of bonded composite joints. Part1: testing and fractography.* Compos Part A 2001; 32:45-58

14. Ashcroft I.A., *A simple model to predict crack growth in bonded joints and laminates under variable-amplitude fatigue*. J. Strain Analysis. 2004;39(6): 707-716

15. Hiley M.J., Dong L., Harding J.,*Effect of strain rate on the fracture process in interlaminar shear specimens of carbon fibre-reinforced laminates*. Compos. Part A. 1997; 28A:171-180

16. Takeshi O., *The fatigue behaviour of toughened epoxy polymers.* Ph.D thesis, Imperial College of Science, London, 1999

17. Li D., Yee A.F., Chen I.-W., Chang S.-C., Takahashi K., *Fracture behaviour of unmodified and rubber-modified epoxy under hydrostatic pressure.* J. Mater. Sci. 1994; 29: 2205-2214

19. Ashcroft I.A., *Fatigue*. In: Adams R.D., editor. Adhesive bonding Science, Technology and Applications, Woodhead Publishing Limited, (2005), p 209-239.